ANGULAR CORRELATIONS BETWEEN INTERNAL CONVERSION ELECTRONS AND GAMMA RAYS IN THE 620 keV CASCADE OF Ba^{131}

A Thesis

submitted to the

Faculty of Graduate Studies

at the

University of Manitoba

in partial fulfillment of the

requirements for the degree of

MASTER OF SCIENCE

by

DONALD A. DOHAN

Winnipeg, Canada

July, 1966

TABLE OF CONTENTS

LIST OF FIGURES

LIST OF TABLES

ACKNOWLEDGEMENTS

This thesis is based on work carried out at the University of Manitoba from May 1965 to June 1966.

The author wishes to express his sincere thanks to the director of the research - Dr. S. K. Sen - for his invaluable encouragement and extremely enthusiastic supervision throughout this work. His assistance in taking some of the data, without which the experiment would have been impossible, is gratefully acknowledged.

The work was supported by the National Research Council of Canada.

ABSTRACT

Systems for high resolution conversion electron and gamma ray detection are described. Results are given for Bi^{207} and Ba^{131}. Measurements on the K/L and K/(L + M) ratios for the 570 and 1064 keV transitions of Bi^{207} yielded the following values :

$(K/L)_{570} = 3.3 \pm 0.3$ $\quad$ $(K/(L + M))_{570} = 2.5 \pm 0.3$

$(K/L)_{1064} = 3.9 \pm 0.3$ $\quad$ $(K/(L + M))_{1064} = 3.0 \pm 0.3$

These measurements are in agreement with an E2 assignment for the 570 keV transition and an M4 assignment for the 1064 keV transition, which give theoretical K/L ratios of 3.4 and 3.7 respectively.

Measurements on the K/(L + M) ratios for the 1046, 922, 620, 496, 373, 216 and 124 keV transitions of Ba^{131} yielded the following values :

$(K/(L + M))_{1046} = 5.8 \pm 0.7$ $\quad$ $(K/(L + M))_{922} = 5.2 \pm 0.5$

$(K/(L + M))_{620} = 5.9 \pm 0.4$ $\quad$ $(K/(L + M))_{496} = 5.9 \pm 0.3$

$(K/(L + M))_{373} = 4.1 \pm 0.3$ $\quad$ $(K/(L + M))_{216} = 3.2 \pm 0.4$

$(K/(L + M))_{216} = 2.3 \pm 0.3$

An internal conversion electron-gamma ray angular correlation spectrometer is described, in which a solid state detector is used for electron detection. Advantages for

performing electron-gamma angular correlation experiments are discussed. The system has been applied in measuring the 620-124-0 cascade angular correlation in Ba^{131} for both the electron-gamma and gamma-electron cases. The values obtained for the coefficients .

$$A_{22} = -0.01 \pm 0.01 \; ; \; A_{44} = -0.02 \pm 0.02 \text{ (gamma-electron)}$$

$$A_{22} = -0.10 \pm 0.03 \; ; \; A_{44} = -0.12 \pm 0.04 \text{ (electron-gamma)}$$

indicate a spin sequence of $\frac{5}{2}^{+} \rightarrow \frac{7}{2}^{+} \rightarrow \frac{5}{2}^{+}$ for the cascade.

INTRODUCTION

In the attempt to construct a logical and satisfying nuclear theory a fairly disperse group of nuclear phenomena has been studied in the last half century. Nuclear structure, and the quantum mechanical properties of the nuclear ground states and excited levels constitute the most important and by far the largest field of investigation. In recent years, many different methods of approach have been developed quite extensively to achieve this.

Electron-gamma angular correlation experiments, which are closely related to the conventional gamma-gamma directional correlations, have recently become subject to a great deal of interest as a technique of nuclear spectroscopy. The information provided by electron-gamma experiments, allows us to determine the multipolarities and mixing ratios of the nuclear transitions. From this we are able to decide about the spins of the excited nuclear energy levels. Contrary to gamma-gamma correlations, electron-gamma experiments distinguish between electric and magnetic characters. Hence we are able to obtain not only the spin but also the parity change caused by the nuclear transition. Another desirable feature of electron-gamma directional correlation measurements is that they are sometimes even more sensitive to minute admixtures of multipole radiations than are the gamma-gamma correlations. Electron-gamma correlations also yield information about the particle

parameters and conversion coefficients, which is important in internal conversion theory. The correlation, in some cases, may be perturbed by electric and magnetic fields acting on the electric and magnetic moments of the nuclei. These fields may, at least in principle, be calculated, or in the case of the magnetic field, externally applied, and hence it is possible to measure magnetic moments and electric quadrupole coupling energies of excited states from the electron-gamma angular correlation experiments.

The electron-gamma angular correlation measurement described in this thesis utilizes a solid state detector for electron detection and a NaI scintillation counter for gamma ray detection. The solid state detector has the following advantages over the usual method employing a beta-ray spectrometer :

1. A solid state detector enables the simultaneous measurement of gamma - K conversion electron and gamma - L conversion electron correlations.
2. The size and geometrical contruction of solid state detectors allow convenient and well defined solid angle corrections.

Other experimental advantages of electron-gamma angular measurements are :

1. The detectors (solid state for electron and NaI crystals for gamma detection) act as particle identifiers. This reduces interference between counters, such as back scattering and Compton events, which may distort the angular correlation.
2. Solid state electron detectors have high detection efficiencies and are capable of much better energy resolution than obtained in gamma-gamma experiments using NaI crystals.

Recently, the theoretical values of the particle parameters for the L conversion electrons have been published. This enables one to obtain another piece of information concerning the nuclear cascade.

ANGULAR CORRELATIONS

Since the introduction, in 1940 (1) of the study of angular correlations of gamma rays in cascade, a great deal of progress has been made in this field especially with the advent of scintillation counters. Many theoretical and experimental papers have since been written on the subject, which is now quite well developed.

The reader is referred to the literature (2) for a detailed description of the theory. The results of the theory for gamma-gamma angular correlation will be summarized and extended to the electron-gamma case.

THE THEORY OF ANGULAR CORRELATIONS

The probability of emission of a particle or quantum by a radioactive nucleus depends, in general, on the angle between the nuclear spin axis and the direction of emission. Specifically, we pick out only those nuclei whose spins lie in a preferred direction. Figure 1 shows a typical angular correlation experiment.

The observation of radiation R_1 in a fixed direction $\underline{k}_1$ selects an ensemble of nuclei that has a nonisotropic distribution of spin orientations. The succeeding radiation

Figure 1 : Angular Correlation Experiment

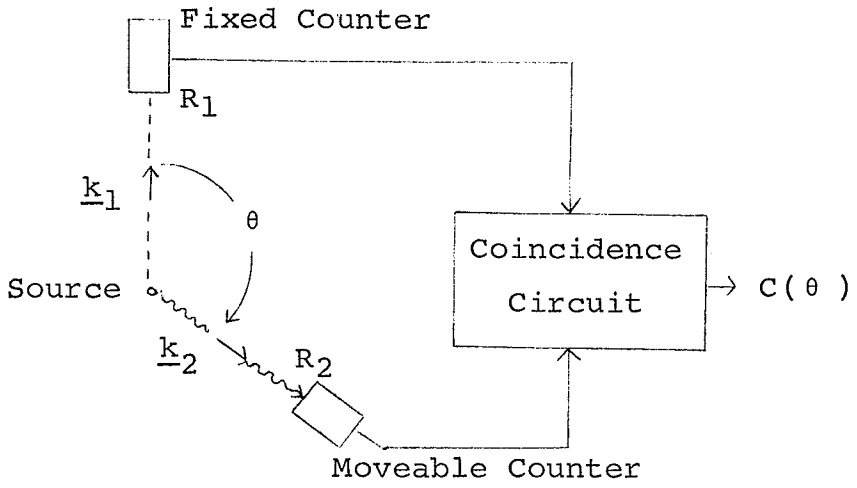

R_2, in direction $\underline{k}_2$, then shows a definite angular correlation with respect to $\underline{k}_1$. Consider the figure below :

Figure 2 : Simple Cascade

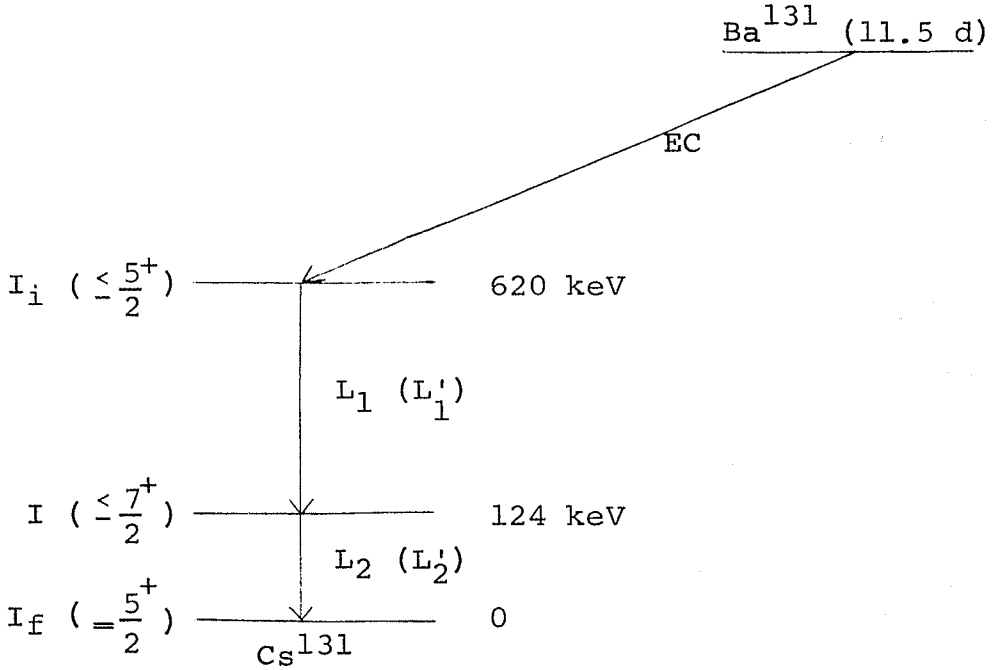

A nucleus, (in our case, Ba^{131}), decays to an excited state of its daughter nucleus, (here the 620 keV level of Cs^{131}). The excited nucleus, in the initial state of spin I_i, decays to an intermediate state, with spin I, by emission of a gamma ray, or a conversion electron. This is followed by another transition, in cascade, to the final state, of spin I_f. The transitions are classified according to the amount of angular momentum, L, carried away by the emitted particle or quantum. The radiation is, then, called a 2^L- pole radiation. Again, for each value of L there are two different types of transitions - electric or magnetic depending on the change of the nuclear parity. The radiation is electric for even L with no change of parity, and for odd L with change in parity. A magnetic transition occurs for even L if there is a change in the nuclear parity or for odd L if the nuclear parity is unchanged. This is summarized as follows :

Angular Momentum (L) Carried Away (Multiple Order of the Radiation	Parity Change	Type of Radiation
0	No	E0 (electric monopole)
1	Yes	E1 (electric dipole)
1	No	M1 (magnetic dipole)
2	No	E2 (electric quadrupole)
2	Yes	M2 (magnetic quadrupole)
3	Yes	E3 (electric octopole)
3	No	M3 (magnetic octopole)

and so on.

The total angular momentum is conserved between the gamma ray and the emitting (or absorbing) system so that if I_i and I_f are the initial and final state spins of the nuclear levels which give rise to the gamma radiations, the angular momentum carried by the gamma ray is given by the rules of addition of angular momentum :

$$|I_i - I_f| \leq L \leq |I_i + I_f|$$

It follows from the above that the transition between two excited nuclear levels may be of a mixed character. That is, the orbital angular momentum carried away by the emitted particle may be either L or L', (usually L' = L + 1).
The mixing ratio for the transition is defined by,

$$\delta^2 = \frac{\text{Number of L' - pole gamma rays}}{\text{Number of L - pole gamma rays}}$$

Referring to Figure 1, if we consider the direction of emission of the first gamma ray as fixed in space, then the probability of emission of the second gamma ray as a function of the angle θ between the gamma ray directions can be expanded in a series of Legendre Polynomials in cos θ :

$$W(\theta) = 1 + A_{22} P_2 (\cos\theta) + A_{44} P_4 (\cos\theta) + \ldots + A_{mm} P_m (\cos\theta)$$

where the value of m which terminates the series is given by the rule :

$m \geq 2I, 2L_1, 2L_2$ where I is the spin of the intermediate state.

The coefficients $A_{\nu\nu}$ are the product of two factors. Each factor corresponds to only one transition of the cascade and is a function of the multipolarity of the transition and the spins of the states involved in the transition. Thus if the two transitions are pure, and are of multipole order L_1 and L_2 respectively, then

$$A_{\nu\nu} = F_\nu (L_1 L_1 I_i I) \; F_\nu (L_2 L_2 I_f I)$$

If, however, one of the transitions, say the first, is mixed, then the F coefficient for the transition, $F_\nu (L_1 L_1 I_i I)$ is replaced by a function containing the mixing ratio of the transitions given by,

$$\frac{F_\nu (L_1 L_1 I_i I) + 2\,\delta_1(\gamma_1)\; F_\nu (L_1 L_1' I_i I) + \delta_1^2(\gamma_1)\; F_\nu (L_1' L_1' I_i I)}{1 + \delta_1^2 (\gamma_1)}$$

where $\delta_1^2 (\gamma_1)$, as previously described, is the mixing ratio of the first transition. If the second transition is also mixed, a similar expression involving the mixing ratio δ_2 of the second transition can be written.

The F coefficients have been calculated by Biedenharn and Rose (3) and have been tabulated by Ferentz and Rosensweig (4).

We have thus far discussed gamma-gamma angular correlations. In the following paragraphs we shall briefly discuss the theory underlying conversion electron - gamma angular correlation measurements. The relativistic theory of the directional correlations involving conversion electrons is due to Rose,

Biedenharn and Arfken (5). Since one of the gamma rays, of multipole order L, is now replaced by a conversion electron, (say a K conversion electron), the corresponding F coefficient for the electron becomes :

$$F_\nu(e) = \alpha_K\, b_\nu(LL)\, F_\nu(LLI_iI)$$

where α_K is the K conversion coefficient for the transition, and b_ν is the K electron particle parameter.

If the converted transition is mixed, the coefficient $F_\nu(e)$ is written as

$$\frac{b_\nu(LL)\, F_\nu(LLI_iI) + 2p(e)\, b_\nu(LL')\, F_\nu(LL'I_iI) + p^2(e) b_\nu(L'L')F_\nu(L'L'I_iI)}{1 + p^2(e)}$$

Here, $p^2(e)$ is the mixing ratio defined by

$$p^2(e) = \frac{\text{Number of L'- pole electrons}}{\text{Number of L - pole electrons}}$$

and is numerically equal to

$$p(e) = \delta(\gamma)\sqrt{\frac{\alpha_K(L')}{\alpha_K(L)}}$$

where the α_K's are the K conversion coefficients of the two multipolarities, L' and L.

Experimentally, we find the number of coincidences between the conversion electrons and the cascade gamma rays as a function of the angle between the directions of emission of the two particles. The curve,

$$W(\theta) = \sum_{\nu=1}^{m} A_{\nu\nu} P_\nu (\cos\theta)$$

is fitted to the data. The coefficients $A_{\nu\nu}$ thus obtained are then compared to theoretical coefficients which have been calculated for various spin assignments of the excited levels and using previously measured mixing ratios for the transitions. In this way, we obtain the spin assignments for the nuclear levels.

EXTRANUCLEAR PERTURBATIONS

It is well known (2) that extranuclear fields can cause strong perturbations of the angular correlation. The nuclear magnetic dipole moment couples to external magnetic fields and the nuclear quadrupole moment will cause a similar coupling to electric field gradients. In both cases, the coupling results in a precession of the nucleus around the external field gradient axis. If the coupling is sufficiently strong, the nuclei change their initial orientations resulting in an attenuation of the angular correlation. Quantum mechanically, if the quantization axis were chosen to coincide with the direction of the first radiation, then the extranuclear interactions cause transitions among the m-states. That is, projections of the nuclear angular momentum along the axis of quantization can undergo transitions.

It has also been proposed (2) that a time-dependent hyperfine structure interaction might appear due to a coupling between the nucleus and the atomic core, which as a result of the preceding K conversion will be in an excited and heavily ionized state. As a consequence, the nucleus is exposed to a strong magnetic field and the nuclear spin will precess about the atomic spin. This difficulty can be overcome by mounting the source on an electrically conducting backing, for which the recovery time of the atomic shell is too short to allow for any attenuation of the angular correlation pattern.

When these extranuclear effects are taken into account, the appropriate theoretical expression then becomes :

$$A_{\nu\nu}^{exp} = G_{\nu}(Q)G_{\nu}(hfs)A_{\nu\nu}^{unperturbed}$$

where $G_{\nu}(Q)$ represents the attenuation due to the static quadrupole interaction and $G_{\nu}(hfs)$ is the attenuation due to the hfs interaction mentioned above. For metallic source environments, $G_{\nu}(hfs) \simeq 1$.

APPARATUS

DETECTORS

The electron detector was a gold-silicon surface barrier p-n junction type obtained from ORTEC. It has a circular area of 50 mm^2 and the depletion depth at a bias of 475 volts was 1500 microns which is the range of a 980 keV electron in silicon. For singles counts, the pulses from solid state detector were led through the low noise Nuclear Enterprises' 5231 preamplifier and were further amplified by a Nuclear Enterprises' 5230 RC amplifier. In the coincidence work, the output pulse from the preamplifier was also fed simultaneously into an ORTEC 203 amplifier which produces double decay line clipped pulses necessary to drive a crossover pick-off unit. At room temperature the system is capable of an energy resolution of 10 keV. For the angular correlation experiment, the detector was cooled to liquid nitrogen temperature, giving a total energy resolution of about 5 keV for the system.

For the gamma spectra of Bi^{207} and Ba^{131}, a Ge(Li) gamma ray detector was used. This was a 2 mm depletion depth by 2.78 cm^2 active area device obtained from R.C.A. These pulses were amplified by a Nuclear Enterprises' 5231-5230 amplifying system. The detector and amplifying system were capable of a total energy resolution (F W H M) of 4.2 keV. at 660 keV.

In the angular correlation work, a 1½" x 1" NaI(Tl) crystal mounted in an integral line assembly with a Dumont 6292 photoumltiplier tube was used for the gamma ray detection. Pulses from this unit were fed, via a cathode follower, to a Nuclear Enterprises' 5202 double delay line amplifier.

ELECTRONICS

The block diagram for the electronics is given in Figure 3. The function of the apparatus was to select those pulses of the correct energy from the detector which were in coincidence with a detected gamma ray, also of the correct energy. These electron pulses were then analyzed in a Nuclear Data 1024 channel analyzer and from this data, the angular correlation function was obtained.

The pulses obtained from the electron and gamma ray detectors, (see the block diagram), after being amplified by the double delay line amplifiers, are fed into two single channel analyzers. The windows of the single channel analyzers were set to accept the appropriate electron and gamma ray energies of the particular cascade. The output pulses of the single channel analyzers, which were initiated at the cross-over point of the double delay line pulses, are fed into a time-to-amplitude converter (TAC) type fast coincidence system. The TAC gives an output pulse whose amplitude is proportional to the time difference between the two input pulses. These output pulses are fed through a single channel analyzer, which

FIGURE 3

Schematic Block Diagram

BLOCK DIAGRAM

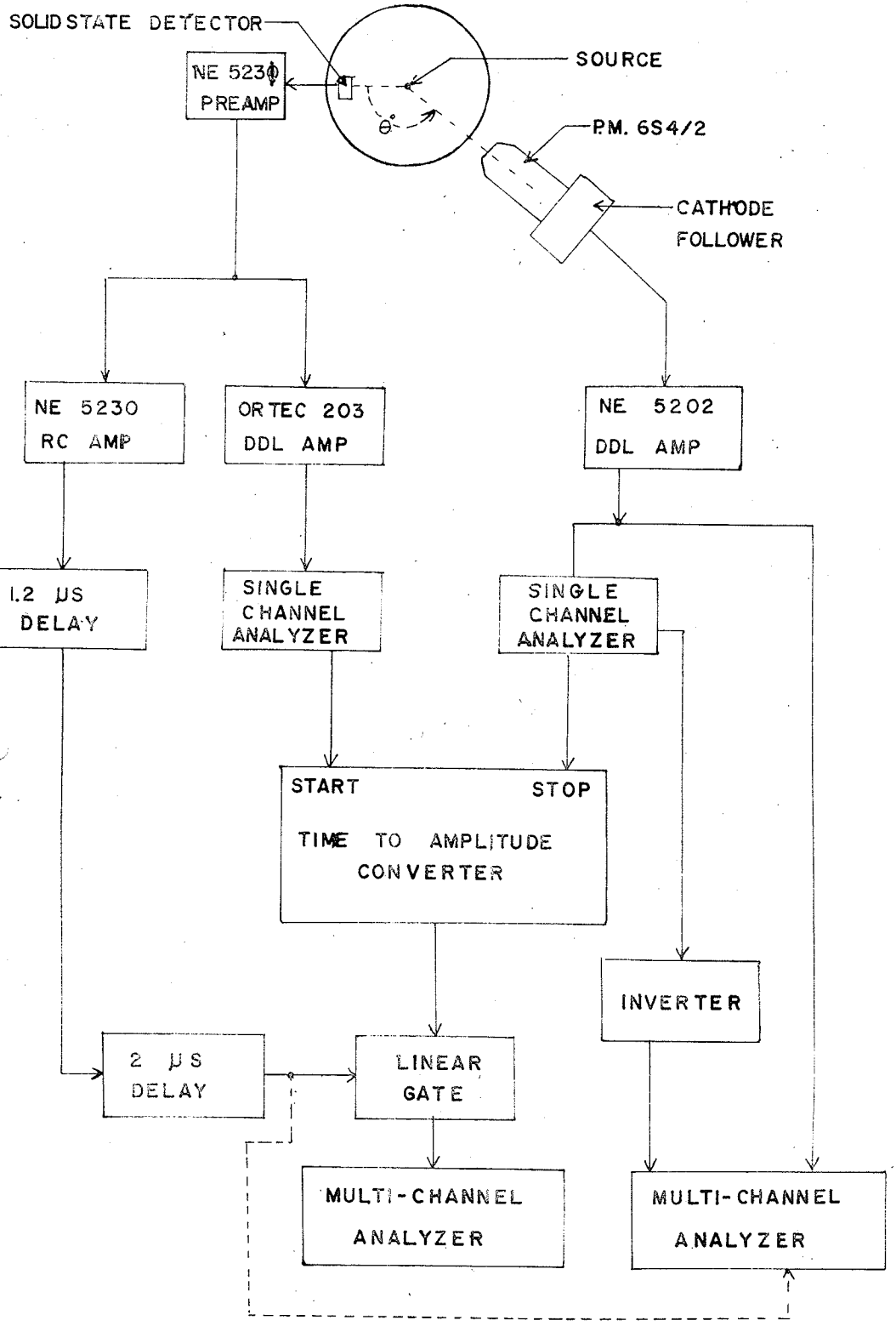

accepts only those pulses which have the correct amplitude, corresponding to the coincidence events. A typical TAC spectrum, showing the single channel analyzer settings is illustrated in Figure 4. The dotted line represents the background due to chance events, which occur randomly in time. The output pulse from the TAC is used to gate the 1024 channel analyzer which analyzes the electron pulses obtained from the good resolution RC amplifier. The coincidence rate was thus taken at several angles to obtain the angular distribution curve. Simultaneously, the single channel analyzer output was used to gate another multichannel analyzer, which accumulated the gamma ray singles spectrum that was allowed through the window of the single channel analyzer. The singles counting rate of the moveable gamma counter was used to normalize the coincidence counting rate at each angle. This is to correct for the finite size of the source and for the possibility of the source not being in the exact center of the arc described by the gamma counter.

SOURCES

Our choice of source was limited by the following considerations :

1. We required a source which decayed by 100% electron capture so that there would be no background beta radiation. The presence of this radiation would make background subtraction extremely difficult.

FIGURE 4

TAC Output

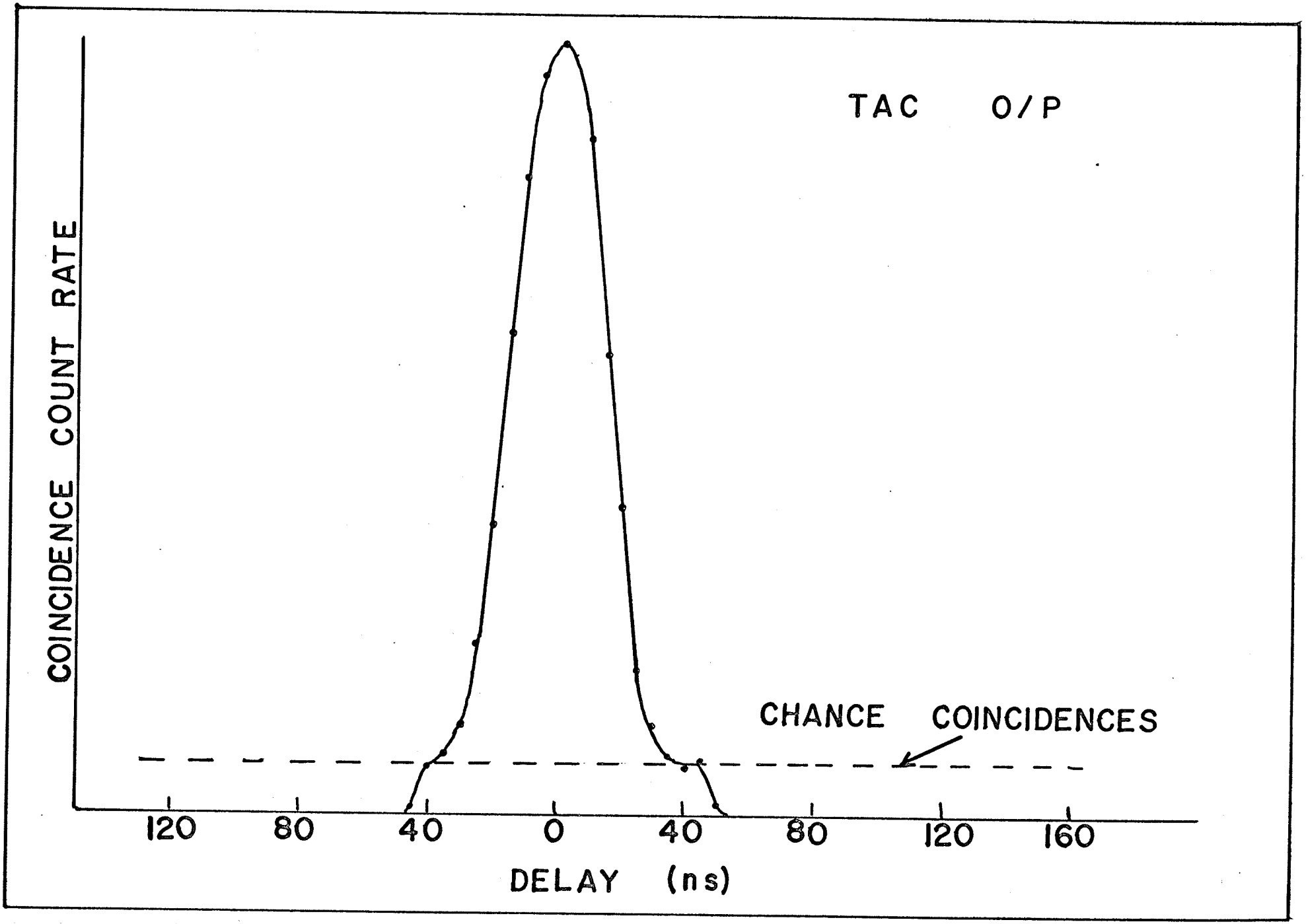
TAC O/P
COINCIDENCE COUNT RATE
CHANCE COINCIDENCES
120
80
40
0
40
80
120
160
DELAY (ns)

2. The conversion electrons should have energies within the energy range from 50 to 1000 keV. The lower limit is due to the rapid build up of pulses due to the backscattering of the electrons from the detector and thus distorting the conversion peak. The upper limit is set by the depletion depth of the detector. Also, in this region, the internal conversion coefficients become quite low thereby greatly reducing the coincidence counting rate.

3. The transition energies should differ sufficiently in order that the conversion lines could be separated in interfering cascades.

Two sources chosen were Bi^{207} (28 years) and Ba^{131} (11.5 days), which decay by electron capture to excited states of Pb^{207} and Cs^{131} respectively. Bi^{207} is a well known source and was used as a calibration in the singles work. In the past, several gamma-gamma angular correlations have been performed on Ba^{131} but the results do not agree well. To our knowledge there has been no measurement on the electron-gamma angular correlation of Ba^{131}. The present work was carried on with much improved resolution in the electron channel in order to remove some of the ambiguities of the earlier work and also to provide new information on this cascade.

For the Bi^{207} work, we used a 1 microcurie source which was depositied on 0.001" thick plastic to minimize scattering.

A preliminary experiment was carried out to measure the 496 gamma - 124 K electron angular correlation in Ba^{131} and in that experiment, the source consisted of a drop of radioactive source solution dried at the centre of a gold plated V.Y.N.S. film which was supported on an aluminum planchette ring.

However, in the final run, in which both the 496 gamma - 124 K electron and the 496 K electron - 124 gamma correlations were measured, the source was sublimed onto a 180 microgram/cm^2 Al foil.

EXPERIMENTAL CHAMBER

The experimental chamber is shown in Figure 5. The chamber is constructed with cylindrical symmetry about the axis of rotation of the moveable scintillation counter. This is to minimize possible anisotropies from being introduced due to scattering. The aluminum planchette source rings were held vertically in the geometrical centre of the vacuum chamber 1.7 cm from the solid state electron detector. Figure 5 also illustrates the mounting of the electron detector of the cold finger of the cryostat. This cold finger is readily interchangeable for various sizes of detectors. The chamber was evacuated by a Balzers rotary pump and a liquid nitrogen cold trap was used to prevent oil vapours from entering the chamber containing the detector and the source. A constant check was made on the temperature of the detector using a thermocouple and of the vacuum in the chamber during the runs.

FIGURE 5

APPARATUS

a - Angular correlation table

b - Vacuum chamber, coldfinger and detector mount

a

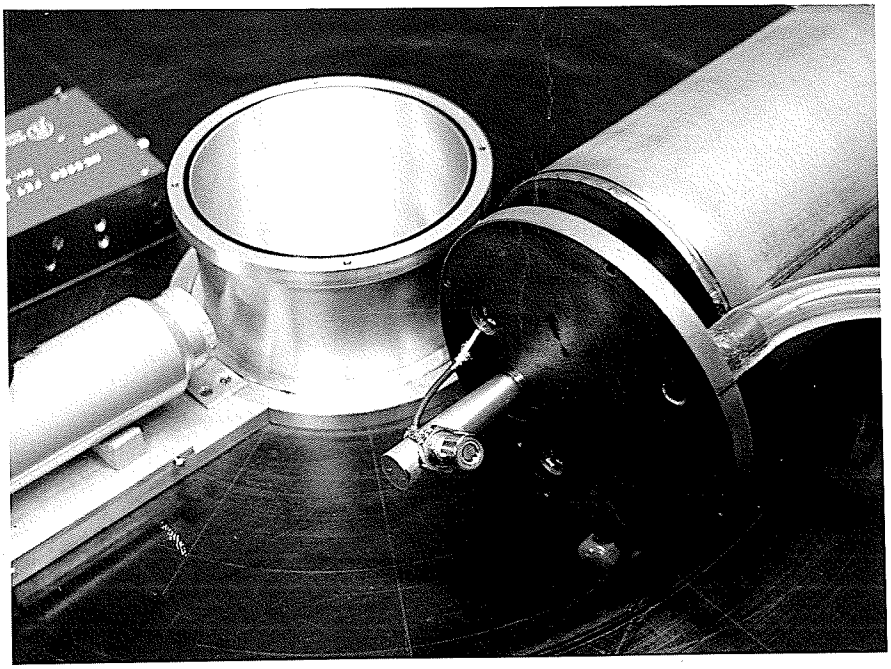

b

RESULTS ON Bi^{207}

The presently accepted level scheme (6) for Bi^{207} is given in Figure 6. The 570 and 1064 keV transitions were investigated using the solid state devices mentioned earlier.

The Bi^{207} gamma singles spectrum is shown in Figure 7. The 6 keV resolution obtained at the 1064 keV peak is slightly greater than that obtained with Ba^{131} reported later. This was because the Ge(Li) detector had warmed up due to a failure in the vacuum system with a resulting decrease in the resolution.

The electron singles spectrum of Bi^{207} is shown in Figure 6. The spectrum was taken with an ORTEC Au - Si surface barrier diode with an applied bias of 475 volts, which corresponds to the range of a 980 keV electron in silicon. It might be possible that the K electrons (976 keV) of the 1064 keV transition were totally absorbed by the detector, while the L electrons (1049 keV) of the same transition might not all be absorbed. In that case the efficiencies for the K and L electrons could be significantly different. In order to decide this, another singles spectrum was run with a Si(Li) detector whose depletion depth corresponds to the range of a 2 MeV electron in silicon. These results were consistent with those obtained using the ORTEC detector.

The K/L and K/(L + M) conversion ratios for the transitions of Bi^{207} are given in Table 1. In column 4 of Table 1 are given

FIGURE 6

Decay Scheme (6) of $Bi^{207} \rightarrow Pb^{207}$

Numbers denote energies in keV

Bi^{207} (28Y)

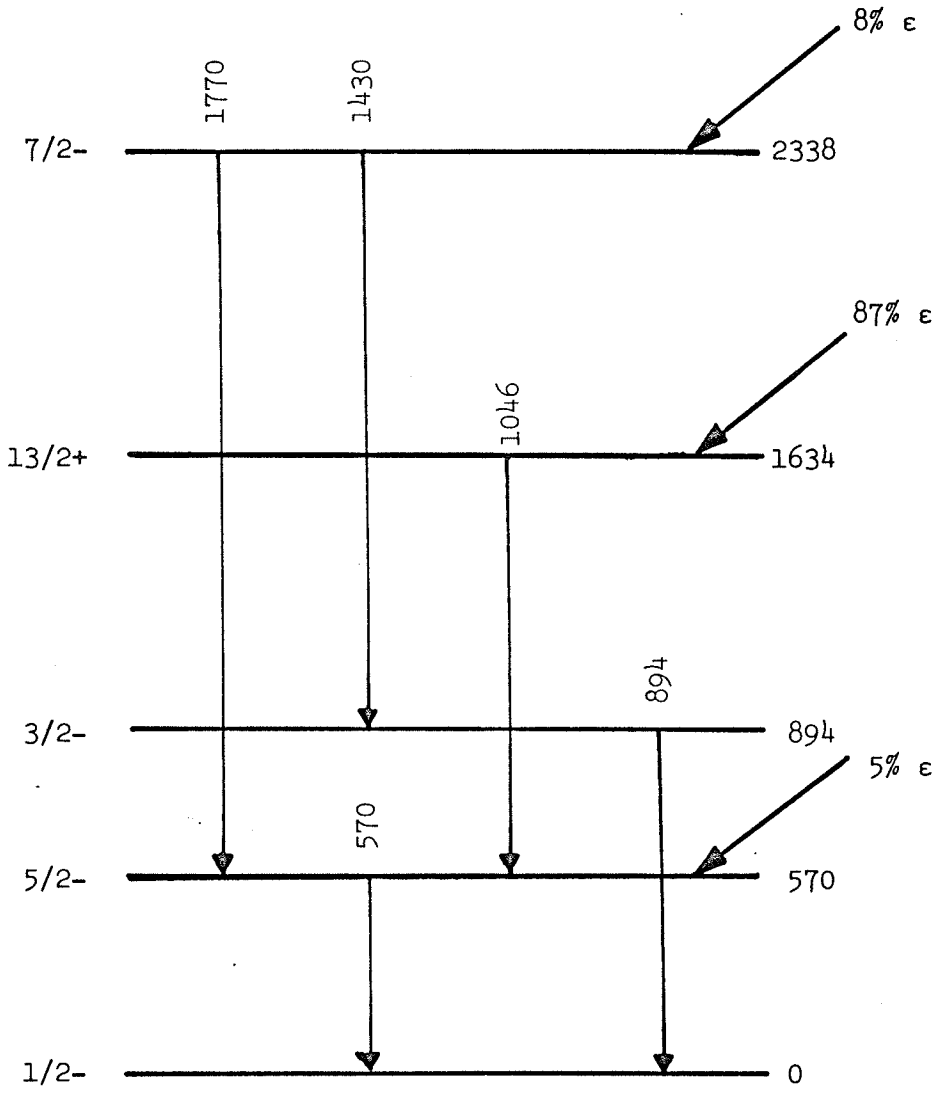

Pb^{207}

FIGURE 7

Bi^{207} Gamma Spectrum

Numbers denote peak energies in keV

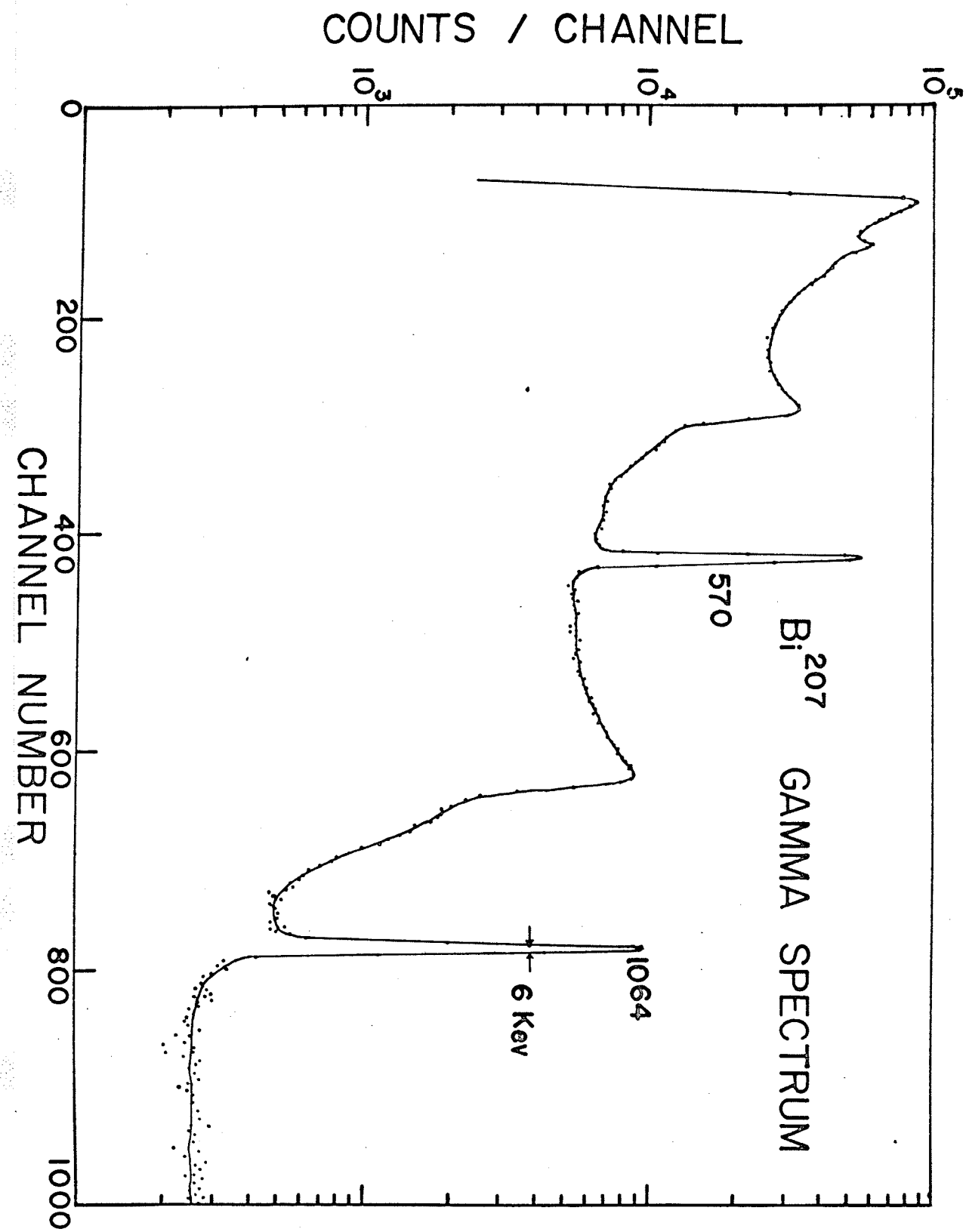
COUNTS / CHANNEL
10^3
10^4
10^5
0
200
400
600
800
1000
CHANNEL NUMBER
Bi^{207} GAMMA SPECTRUM
570
1064
6 Kev

FIGURE 8

Conversion Electron Spectrum of Bi^{207}

Numbers denote transition energies in keV

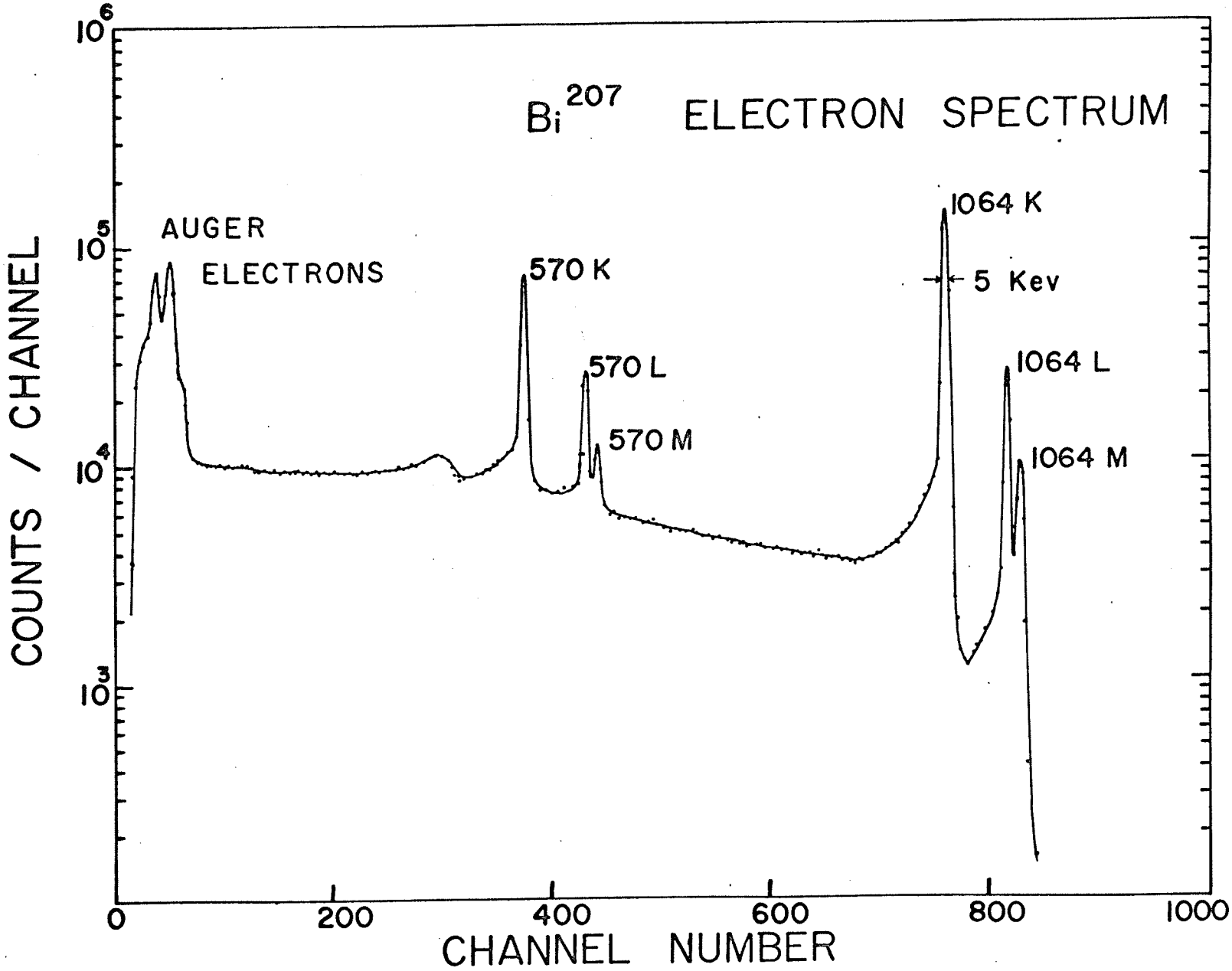
Bi 207 ELECTRON SPECTRUM
AUGER ELECTRONS
570 K
570 L
570 M
1064 K
5 Kev
1064 L
1064 M
COUNTS / CHANNEL
CHANNEL NUMBER
10^6
10^5
10^4
10^3
0
200
400
600
800
1000

TABLE 1

K/L and K/(L + M) Conversion Ratios in Pb^{207}

Quantity	Alburger and Sunyar	Kurey and Roy	Present Work	Theoretical Values
K/L_{570}	3.4 ± 0.4	-	3.3 ± 0.3	3.4
K/L_{1064}	3.95 ± 0.25	-	3.9 ± 0.3	3.7
$K/(L + M)_{570}$	-	3.11 ± 0.11	2.5 ± 0.3	-
$K/(L + M)_{1064}$	-	4.34 ± 0.17	3.0 ± 0.3	-

the theoretical values for the K/L ratios which were obtained from graphical interpolation of internal conversion coefficients calculated by Rose (7), assuming an M4 assignment for the 1064 keV transition, and an E2 assignment for the 570 keV transition. Our values of 3.3 ± 0.3 and 3.9 ± 0.3 for the K/L ratios of the 570 keV and 1064 keV transitions respectively are in good agreement with the measurements of Alburger and Sunyar (6). Our K/(L + M) ratio measurements do not, however, agree within the experimental errors with the values obtained by Kurey and Roy (8) who encountered the difficulty, mentioned above, concerning the depletion depth of the detector.

Comparison of the data with the theoretical values of the internal conversion coefficient ratios indicates good agreement with the E2 assignment for the 570 keV transition and the M4 assignment for the 1064 keV transition.

The errors on the values of the ratios of the conversion coefficients accumulate from the measurement of the relative areas, of the electron singles spectrum. The errors in the areas are limited to 4% or less by repeated measurements.

RESULTS ON Ba^{131}

SINGLES

The presently accepted level scheme (9) for Ba^{131} decaying to Cs^{131} is shown in Figure 9. The cascades investigated were those between the 620 keV level and the ground state.

The gamma ray singles spectrum of Ba^{131} taken with the Ge(Li) detector is given in Figure 10. We were able to identify 27 of the 32 lines reported earlier (9). We have seen two extra lines, one at 952 keV and the other at 979 keV. They are not shown in the decay scheme of Figure 9 because we have not conclusively proved that they belong to Ba^{131} although we can say that they do not belong to either Ba^{133m} or Cs^{132} which were present as impurities.

The conversion electron singles spectrum of Ba^{131} taken with the Au-Si surface barrier diode is shown in Figure 11. Of the 32 lines reported earlier (9), we were able to identify 25. The K/(L + M) conversion ratios for the 124, 216, 373, 496, 620, 922 and 1046 keV transitions have been measured. The results are summarized in Table 2. These values are compared with other published values (9), (10), (11). Our values for the first four transitions agree with those of Brundrit and Sen (11) who also performed their measurements using a solid state detector. The L + M 216 line is composite with the K248

FIGURE 9

Decay Scheme (9) of $Ba^{131} \rightarrow Cs^{131}$

Numbers denote energies in keV

Ba^{131} (11.5 d)
2.9% ε
1.0% ε
54.5% ε
1.8% ε
19.3% ε
19.7% ε
1046
696
619
584
373
216
133
124
78
0
1046
923
914
831
674
461
427
350
696
573
480
324
620
496
486
403
246
584
461
452
373
294
248
240
157
216
137
92
82
133
55
124
78
(3/2,5/2+)
(≤5/2+)
(≤5/2+)
(≤5/2+)
(3/2,5/2+)
(3/2,5/2+)
(3/2+)
(<7/2)
(7/2+)
5/2+
Cs^{131}

FIGURE 10

Ba^{131} Gamma Spectrum

Numbers denote peak energies in keV

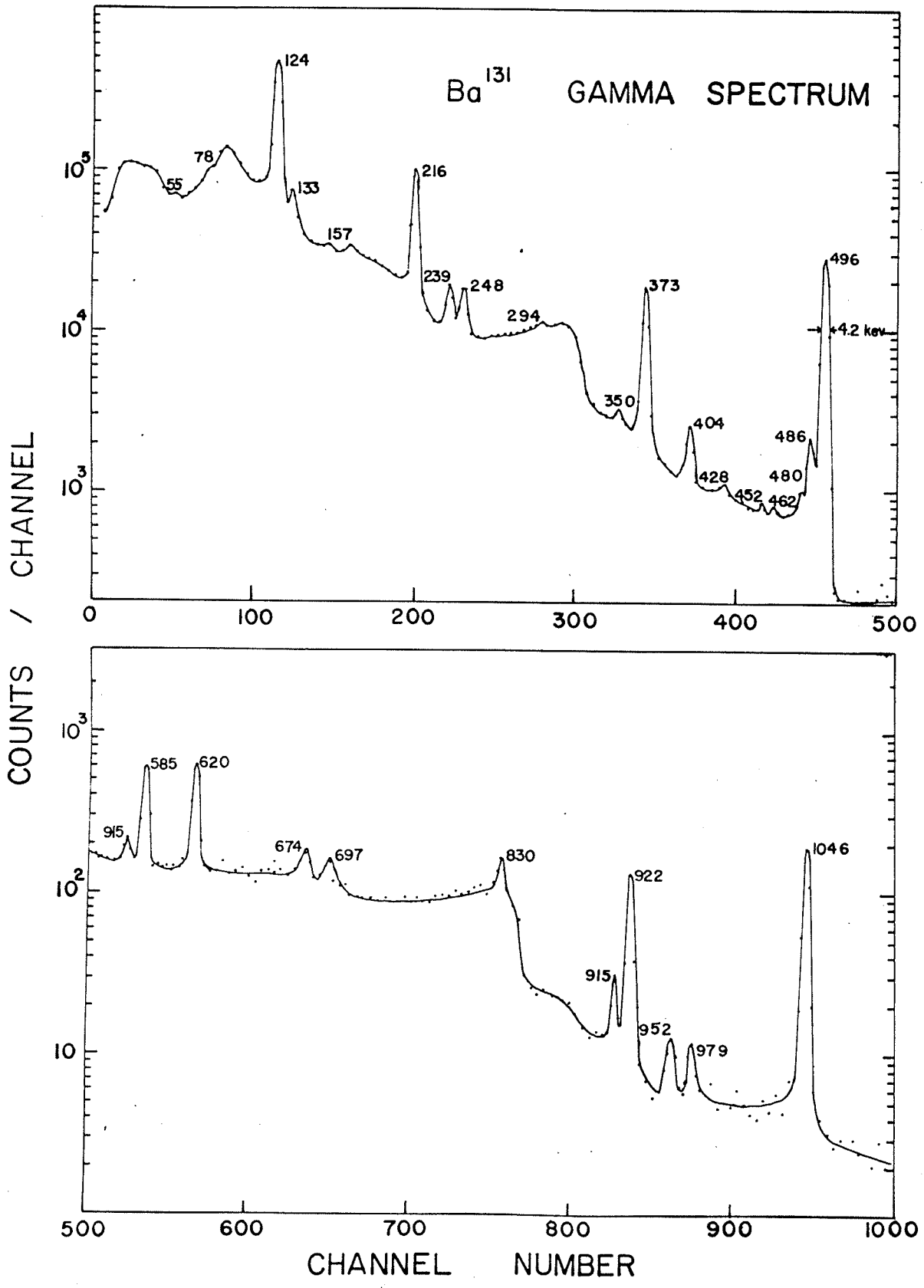
Ba 131 GAMMA SPECTRUM
124
78
55
133
157
216
239
248
294
373
350
404
428
452
462
486
480
496
4.2 kev
COUNTS / CHANNEL
915
585
620
674
697
830
922
915
952
979
1046
CHANNEL NUMBER

FIGURE 11

Conversion Electron Singles Spectrum of Ba^{131}

Numbers denote transition energies in keV

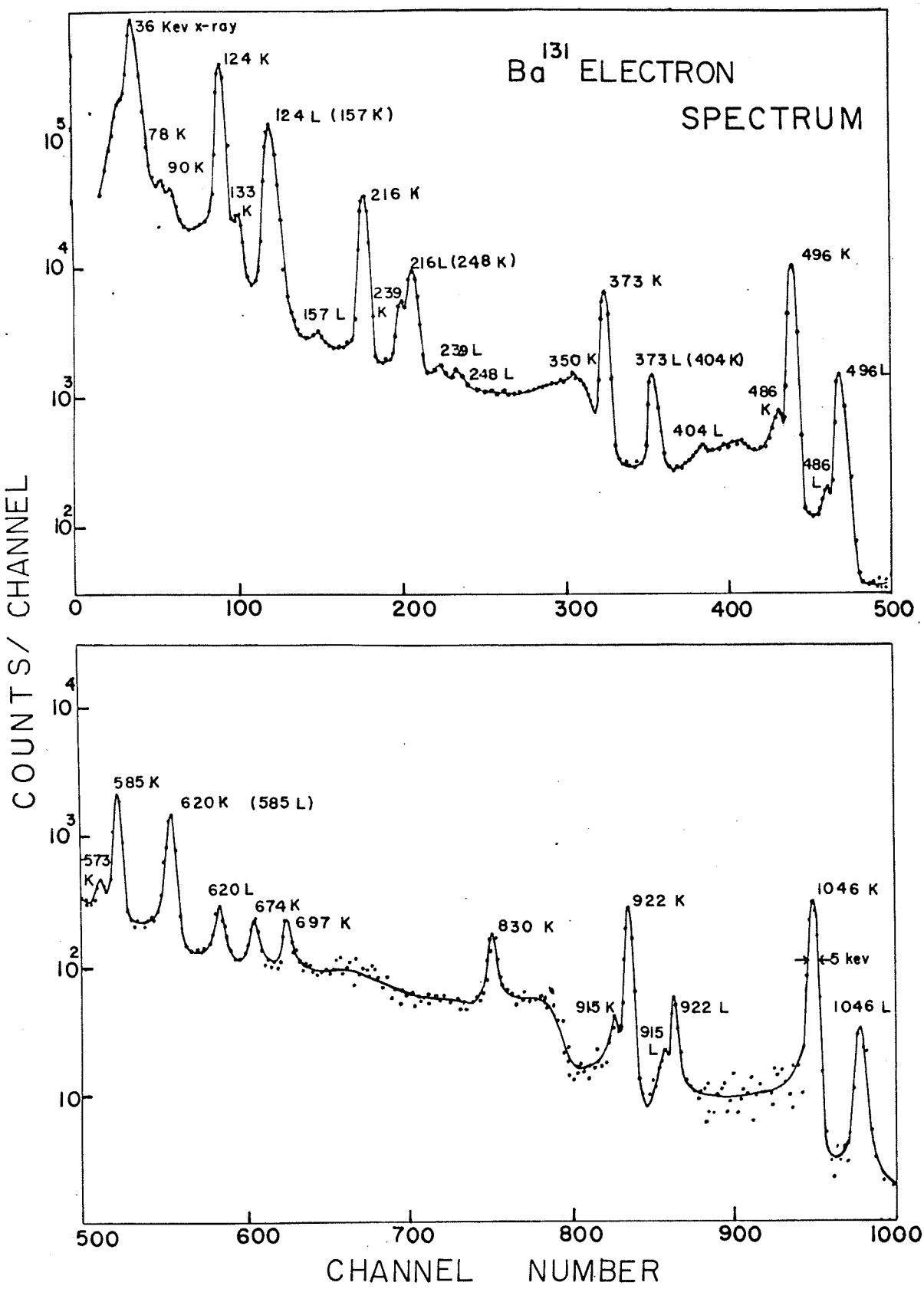
Ba 131 ELECTRON SPECTRUM
36 Kev x-ray
124 K
78 K
90 K
133 K
124 L (157 K)
216 K
157 L
239 K
216L(248 K)
239 L
248 L
350 K
373 K
373 L (404 K)
404 L
486 K
496 K
486 L
496L
585 K
620 K (585 L)
573 K
620 L
674 K
697 K
830 K
915 K
922 K
915 L
922 L
1046 K
1046 L
5 kev
COUNTS/ CHANNEL
CHANNEL NUMBER

TABLE 2

K/(L + M) Conversion Ratios in Cs^{131}

Transition Energy (keV)	Cork et al	Kelly and Horen	Brundrit and Sen	Present Work
124	3.6 ± 0.3	3.0 ± 0.2*	2.7 ± 0.3	2.3 ± 0.3
216	9 ± 2	> 6.7*	3.1 ± 0.3	3.2 ± 0.4⁎
373	6.0 ± 0.5	> 5.0*	4.6 ± 0.5	4.1 ± 0.4‡
496	7.7 ± 0.5	7.3 ± 0.8*	6.2 ± 0.6	5.9 ± 0.3
620	-	10 ± 3	-	5.9 ± 0.5
922	-	9 ± 3	-	5.2 ± 0.5
1046	-	8.4 ± 1.6	-	5.8 ± 0.7

* These values are quoted as K/L in the original papers
⁎ The K 248 is composite with the L + M 216 (See the text)
‡ The K 404 is composite with the L + M 373 (See the text)

line, and its contribution has not been removed. Hence the K/(L + M) ratio for the 216 keV transition is low, in accordance with the result of Kelly and Horen (9). Similarly, the K/(L + M) ratio for the 373 keV line is also low due to the K 404 contribution to the L + M 373 line, which has not been removed.

The errors in the ratios of the conversion coefficients of Ba^{131} were estimated in the same way as in the case of Bi^{207}.

ANGULAR CORRELATION

In the first part of the angular correlation experiment, the windows of the single channel analyzers were set to accept the 496 keV conversion electrons and the 124 keV gamma rays. The TAC discriminators were set to accept the coincidences between these selected pulses. Coincidences were taken for 2 hours and 40 minutes at 15 degree intervals, from 90 degrees to 180 degrees. The complete angular range (in all seven angles) from 90 to 180 degrees was scanned three times alternately in opposite directions. A singles gamma ray spectrum for which the multichannel analyzer was gated with the output of the single channel analyzer was taken at each angle, both before and after the experiment. After the experiment, the discriminators of the TAC were set for a region away from the true coincidence region. In this way, the chance coincidences were subtracted from the true coincidences. In the second part of the experiment, the same procedure was repeated, this time with the single channel

analyzers set to accept the 496 keV gamma ray and the 124 keV conversion electrons respectively. The 124 keV conversion electrons in coincidence with the 496 keV gamma ray and the 496 keV conversion electrons in coincidence with the 124 keV gamma rays are shown in Figure 12. The 133 keV K electron is also present in the coincidence spectrum since it is in coincidence with the 486 keV gamma ray, which we were not able to resolve from the 496 keV line with the scintillation counter. Also evident, in Figure 12, is the 486 keV K conversion electron in coincidence with the 133 keV gamma ray.

The total number of coincidences were found at each angle by subtracting the backscattered contribution from the L + M electrons, and insisting that the peaks be symmetrical. The coincidence counting rate was then normalized to the corresponding singles gamma ray counting rate. The data was then corrected for decay of the source during the experiment. The quantity $W(\theta)/W(90^{o})$ plotted as a function of angle θ for the three experiments is given in Figure 13. The errors indicated in the figure are the statistical errors in the counts at each position.

ANALYSIS OF THE DATA

The data were analyzed by two methods. In the first method, the least squares fit curve to the seven data points was found. In the second method, the data at the points 90^{o}, 135^{o} and 180^{o} were used to solve for the coefficients A_{22} and A_{44} where the

FIGURE 12

Conversion Electron Coincidence Spectrum of Ba^{131}

Numbers denote transition energies in keV

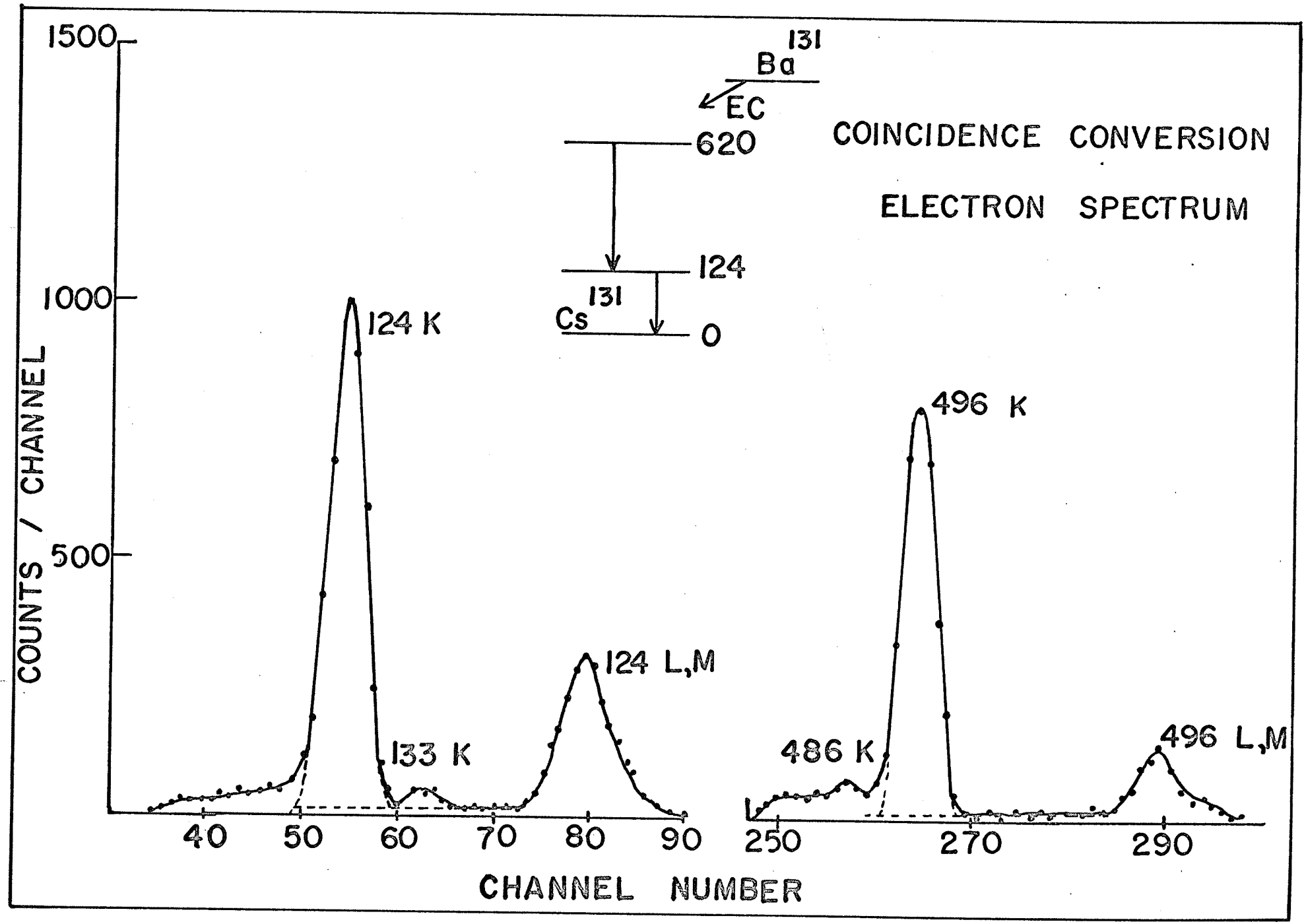
COINCIDENCE CONVERSION
ELECTRON SPECTRUM
^{131}Ba
EC
620
124
^{131}Cs
0
124 K
133 K
124 L,M
496 K
486 K
496 L,M
COUNTS / CHANNEL
CHANNEL NUMBER
1500
1000
500
40
50
60
70
80
90
250
270
290

FIGURE 13

$W(\theta)/W(90)$ vs θ

The dotted lines are the best fit curves to the data

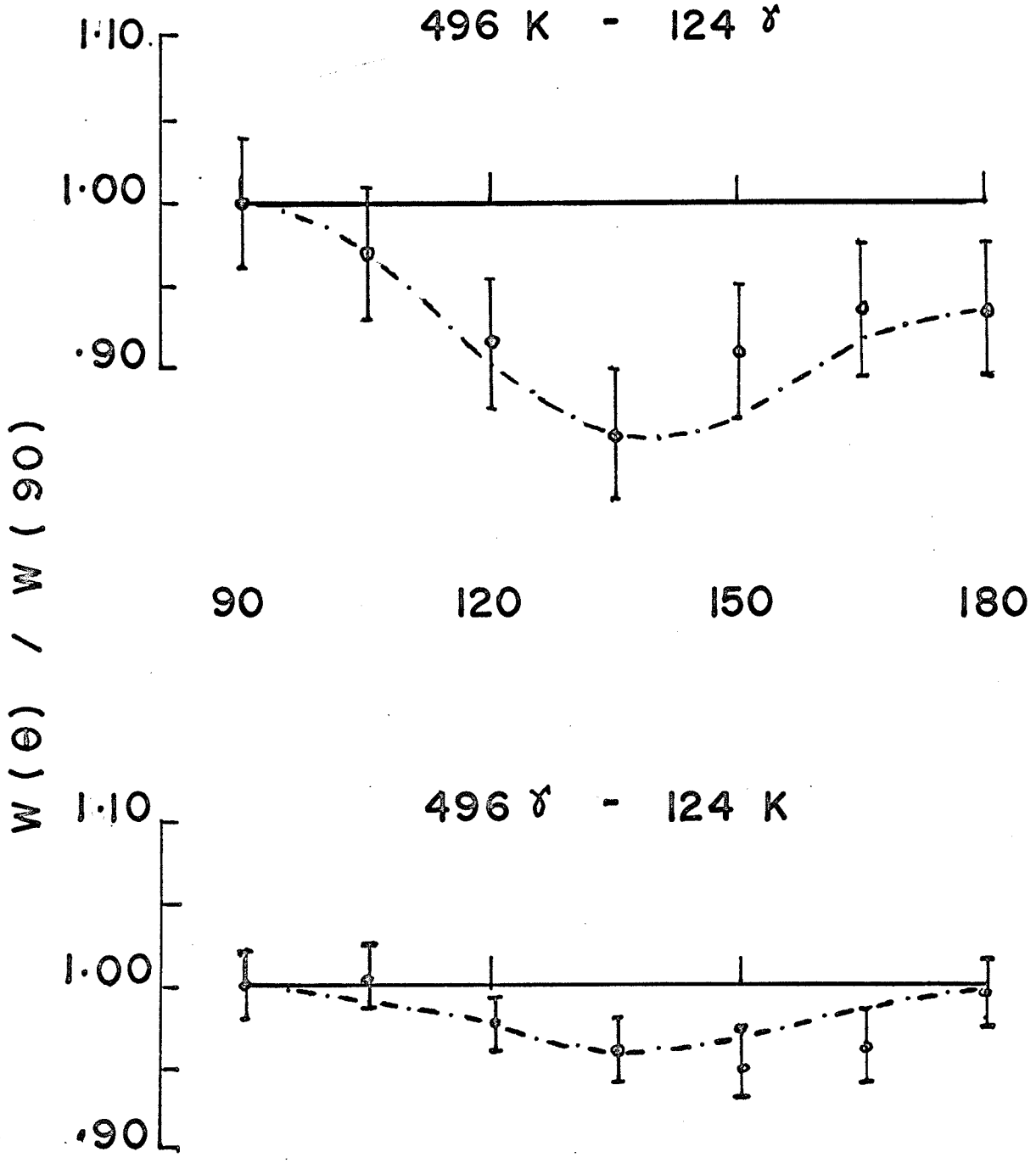
496 K - 124 γ
1·10
1·00
·90
90
120
150
180
W(θ) / W(90)
496 γ - 124 K
1·10
1·00
·90
θ (DEGREES)

first coefficient of the Legendre Polynomial expansion, A_{00}, was normalized to unity. In both cases, the series of Legendre Polynomials was carried to the 4th order since both transitions contain E2 multipole order radiations.

LEAST SQUARES FIT TO THE DATA

The I.B.M. 1620 computer was programmed to compute the least squares fit curve of the seven data points to the function

$$W(\theta) = C_0 + C_2P_2 (\cos\theta) + C_4P_4 (\cos\theta)$$

The program, written Fortran II is given in Appendix A, together with a sample output of the program. The method used in the program gives the least squares fit to the parabola :

$$W(\theta) = a + b \cos^2 (\theta) + c \cos^4 (\theta)$$

and then uses the values of a,b,c, to yield the coefficients C_o, C_2 and C_4. The disadvantage in this method of curve fitting is that the errors obtained in the coefficients are not dependent on the errors obtained in the counting statistics.

METHOD OF WHITE (12)

In this method, White (12) shows that it is sufficient to take the data at $(\frac{1}{2}m + 1)$ angles, where m is the highest order Legendre Polynomial in the expansion of $W(\theta)$. For m = 4, as in our case, White shows that to maximize the efficiency of the statistics, the data should be taken at the angles 90^o, 135^o and 180^o. The experimentally obtained quantities, $W(\theta_i)$, taken at the above mentioned three angles, was used to solve the

system of equations,

$$W(\theta_i) = C_0 + C_2P_2(\cos\theta_i) + C_4P_4(\cos\theta_i), \quad i = 1, 2, 3.$$

The I.B.M. 1620 computer was programmed to compute the coefficients C_2 and C_4 (here C_0 is normalized to unity) and the statistical errors in these coefficients. This program, written in Fortran II is given in Appendix B together with a sample output.

The coefficients obtained from the analysis are given in Table 3. The coefficients have been corrected for finite solid angle using the table of Yates (13). The coefficients thus obtained have been used to calculate the best fit curve at $2\frac{1}{2}^{o}$ intervals. These curves are plotted in Figure 13.

Comparing the signs of the theoretically obtained coefficients given in Table 4 with those of the experimentally achieved coefficients given in Table 3, we can eliminate all spin assignments except for the sequences

$$\frac{5^+}{2} \rightarrow \frac{7^+}{2} \rightarrow \frac{5^+}{2}$$

and

$$\frac{3^+}{2} \rightarrow \frac{3^+}{2} \rightarrow \frac{5^+}{2}$$

On further comparison of the absolute values of the A_{22} coefficients, we find that only the spin sequence of

$$\frac{5^+}{2} \rightarrow \frac{7^+}{2} \rightarrow \frac{5^+}{2}$$

is valid for the cascade. This is substantiated by the fact

TABLE 3

Experimental A_{22} and A_{44} Coefficients

	Electron-Gamma	Gamma-Electron
A_{22}	-0.10 ± 0.03	-0.01 ± 0.01
A_{44}	-0.12 ± 0.04	-0.02 ± 0.02

The quoted errors are statistical only

that while an assignment of $\frac{3^+}{2} \rightarrow \frac{3^+}{2} \rightarrow \frac{5^+}{2}$ gives a zero value for the coefficient A_{44}, experimentally we obtain a non-zero value. This also means that the first transition is not pure M1 but has an admixture of E2 transitions.

The 124 keV state of Ba^{131} has a half-life of $\sim 4 \times 10^{-9}$ sec and hence an attenuation of the angular correlation might be expected due to quadrupole interaction as mentioned earlier in this thesis. We performed the experiments with sources in two different forms so as to introduce quadrupole interaction, if present, in different strengths. However we found that the values of the coefficients (A_{22}, A_{44}) for both cases agreed within the experimental errors, and we therefore, assumed that the attenuation effect, if present, is very small.

INTERPRETATION OF THE RESULTS

From shell model considerations, the spins and parities of Ba^{131} are limited to the values $\leq \frac{5^+}{2}$ for the 620 keV level, and to $\leq \frac{7^+}{2}$ for the 124 keV level. The ground state spin of Cs^{131} is known definitely to be $\frac{5^+}{2}$. From the measurements (9) of K conversion coefficients, the 496 keV transition has been found to be predominantly M1, with a small possible mixture of E2. The K/L conversion coefficient measurement (9) of the 124 keV transition supports an E2 assignment for the transition, with a possible admixture $\sim$ 8% of M1.

The A_{22} coefficients have been calculated for all possible spin assignments for the cascade, within the limits prescribed by the shell model. These coefficients are given in Table 4 and have been calculated using a pure M1 multipolarity assignment for the 496 keV transition, and an 8% admixture of M1 radiation in the predominantly E2 radiation of the 124 keV transition. The values of the particle parameters necessary to determine A_{22} and A_{44} were obtained from graphical extrapolation of the values given in Rose's (3) tables. They are :

	124 keV transition	496 keV transition
b_2^m	0.17	0.49
b_2	0.06	0.51
b_2^e	1.91	1.51

In the above table, the supercript m refers to a magnetic

transition, e refers to an electric transition, and no supercript refers to a mixed transition.

TABLE 4

Theoretical A_{22} Coefficients

Spin Sequence	Electron-Gamma	Gamma-Electron
$\frac{5}{2} \rightarrow \frac{7}{2} \rightarrow \frac{5}{2}$	-0.09	-0.05
$\frac{3}{2} \rightarrow \frac{7}{2} \rightarrow \frac{5}{2}$	0.00	0.00
$\frac{5}{2} \rightarrow \frac{5}{2} \rightarrow \frac{5}{2}$	0.03	-0.14
$\frac{3}{2} \rightarrow \frac{5}{2} \rightarrow \frac{5}{2}$	-0.02	0.12
$\frac{1}{2} \rightarrow \frac{5}{2} \rightarrow \frac{5}{2}$	0.00	0.00
$\frac{5}{2} \rightarrow \frac{3}{2} \rightarrow \frac{5}{2}$	0.04	0.07
$\frac{3}{2} \rightarrow \frac{3}{2} \rightarrow \frac{5}{2}$	-0.14	-0.26
$\frac{1}{2} \rightarrow \frac{3}{2} \rightarrow \frac{5}{2}$	0.14	0.32

APPENDIX A

The program described in this thesis was used in the analysis of the angular correlation data. It is designed to compute the least square fit curve of the seven data points to the function

$$W(\theta) = C_0 + C_2P_2(\cos\theta) + C_4P_4(\cos\theta)$$

The coincidence counting rates at the angles 90°, 105°, 120°, 135°, 150°, 165° and 180° respectively are entered as input data for the program. The data, which has been normalized to unity at 90°, is written in Format F5.3. The present program is designed to accept 15 sets of seven data points.

Since only even powers of $\cos(\theta)$ arise in the Legendre Polynomial expansion of $W(\theta)$, the function can be expanded in the form

$$W(\theta) = a + b\cos^2(\theta) + c\cos^4(\theta)$$

which is the form of a parabola in $\cos^2(\theta)$.

The program performs a standard least square fit to obtain the coefficients a, b, and c. These coefficients are then converted to the quantities C_0 (which is normalized to unity), C_2, and C_4, which can be compared with theoretical values.

The program uses the coefficients to compute the theoretical values of the function at $2\frac{1}{2}^\circ$ intervals. The theoretical curve, together with the experimental points is plotted in the form of an output from the computer.

```
ZZFORX51
*FANDK1604
      DIMENSION X(7),Y(7)
      X(1)=0.000
      X(2)=.0670
      X(3)=.250
      X(4)=.500
      X(5)= .750
      X(6)=.933
      X(7)=1.000
      K=0
      M=1
    3  A=7.
       B=0.
       C=0.
      D=0.
      E=0.
      GO TO (30,32,25),M
   30 PUNCH 31
   31 FORMAT (45H 496 K ELECTRON-124 GAMMA ANGULAR CORRELATION/)
      GO TO 40
   32 PUNCH 33
   33 FORMAT(45H 496 GAMMA-124 K ELECTRON ANGULAR CORRELATION/)
      GO TO 40
   34 PUNCH 35
   35 FORMAT(45H 496 GAMMA-124 L ELECTRON ANGULAR CORRELATION/)
      GO TO 40
   40 K=K+1
      GO TO (28,14,16,18,20),K
   28 PUNCH 2
    2 FORMAT (14H       RUN NO.1/)
      GO TO 42
   14 PUNCH 15
   15 FORMAT (15H       RUN NO. 2/)
      GO TO 42
   16 PUNCH 17
   17 FORMAT (15H       RUN NO. 3/)
      GO TO 42
   18 PUNCH 19
   19 FORMAT (15H       RUN NO. 4/)
      GO TO 42
   20 PUNCH 21
   21 FORMAT (15H       RUN NO. 5/)
   22 M=M+1
      K=0
      GO TO 42
   42 READ 4,(Y(J),J=1,7)
    4 FORMAT (F5.3)
      DO 5 I=1,7
      B=B+X(I)
      C=C+(X(I)*X(I))
      D=D+(X(I)*X(I)*X(I))
    5 E=E+(X(I)*X(I)*X(I)*X(I))
      P=(A*C*E)+((B*D*C)*2.)-(C*C*C)-(D*D*A)-(B*B*E)
      Q=0.
      R=0.
      S=0.
      DO 6 I=1,7
      Q=Q+Y(I)
      R=R+(X(I)*Y(I))
    6 S=S+(X(I)*X(I)*Y(I))
```

```
      T=(Q*C*E)+(R*D*C)+(S*D*B)-((C**2.)*S)-((D**2.)*Q)-(E*R*B)
      U=(A*R*E)+(B*S*C)+(C*D*Q)-(C*R*C)-(D*S*A)-(E*B*Q)
      V=(A*C*S)+(B*D*Q)+(C*R*B)-(C*Q*C)-(R*D*A)-(S*B*B)
      AT=T/P
      BU=U/P
      CV=V/P
      PUNCH 7,AT,BU,CV
    7 FORMAT (3F10.4)
      CALL PLOT (1,90.,180.,9.,1.,.5,1.5,10.,1.)
      Z=0.
      I=0
      AA=75.
    8 I=I+1
      AA=AA+15.
      CALL PLOT (9,AA,Y(I))
      PUNCH 9,I,Y(I)
    9 FORMAT (I6,F10.4)
      AY=AT+(BU*X(I))+(CV*X(I)*X(I))
      ER=(AY-Y(I))*(AY-Y(I))
      Z=Z+ER
      IF (I-7) 8,10,10
   10 EZ=SQRTF(Z/(A-3.))
      T1=SQRTF(((C*E)-(D*D))*((C*E)-(D*D)))
      T2=SQRTF(((A*C)-(C*C))*((A*C)-(C*C)))
      T3=SQRTF(((A*C)-(B*B))*((A*C)-(B*B)))
      EAT=EZ*SQRTF(T1/P)
      EBU=EZ*SQRTF(T2/P)
      ECV=EZ*SQRTF(T3/P)
      PUNCH 7 ,EAT,EBU,ECV
      BB=87.5
   11 BB=BB+2.5
      BBR = BB*6.2832/360.
      BBRC = COSF(BBR)
      BBRD = BBRC*BBRC
      AYC = AT+(BU*BBRD)+(CV*BBRD*BBRD)
      PUNCH 12,BB,AYC
   12 FORMAT(2F10.4)
      CALL PLOT (9,BB,AYC)
      IF (BB-180.) 11,13,13
   13 CONTINUE
      C4= (8./35.*CV)
      C2= (2./3.)*BU+(5./2.*C4)
      CN= AT + (C2/2.)-(3./8.*C4)
      PUNCH 7,CN,C2,C4
      C4E=8./35.*ECV
      C2E= SQRTF((4./9.*EBU*EBU)+(25./4.*C4E*C4E))
      CNE=SQRTF((EAT*EAT)+(1./4.*C2E*C2E)+(9./64.*C4E*C4E))
      CNN=1.
      C2N=C2/CN
      C4N=C4/CN
      PUNCH 7,CNN,C2N,C4N
      PUNCH 7,CNE,C2E,C4E
      N=1
      PUNCH 26,N
   26 FORMAT (I1)
      CALL PLOT (7)
      GO TO 3
   25 CALL EXIT
      END
```

Consider the sample output given on the following page. The output data is given in the following order :

The title of the experiment, which the programmer preselects, is typed out. This is followed by the coefficients a, b, and c. The experimental data (which has previously been read in as input data) is typed out to insure that the proper data has been read in. The integers 1, 2 ... 7 refer to the angles 90^{o}, 105^{o}, ... 180^{o} respectively. Note that the experimental data has been normalized to unity at 90^{o} i.e. (1). The computer errors in a, b, and c follow. The coefficients a, b, and c are used to compute the values of the best fit curve $W(\theta)$ through the data. The angles and the corresponding values of $W(\theta)$ are typed out for the angular range 90^{o} to 180^{o}, at $2\frac{1}{2}^{o}$ intervals. The coefficients C_0, C_2 and C_4 are then given. These are followed by the normalized values. In the final line of the output, the errors in the coefficients C_0, C_2, and C_4 are given.

496 K ELECTRON-124 GAMMA ANGULAR CORRELATION

RUN NO. 2

.9908	-.4356	.3988
1	1.0000	
2	.9810	
3	.8600	
4	.8670	
5	.9450	
6	.9080	
7	.9470	
.0306	.2109	.1632
90.0000	.9908	
92.5000	.9900	
95.0000	.9875	
97.5000	.9835	
100.0000	.9781	
102.5000	.9713	
105.0000	.9634	
107.5000	.9547	
110.0000	.9453	
112.5000	.9356	
115.0000	.9257	
117.5000	.9161	
120.0000	.9068	
122.5000	.8983	
125.0000	.8907	
127.5000	.8841	
130.0000	.8789	
132.5000	.8751	
135.0000	.8727	
137.5000	.8718	
140.0000	.8725	
142.5000	.8746	
145.0000	.8781	
147.5000	.8827	
150.0000	.8884	
152.5000	.8949	
155.0000	.9020	
157.5000	.9095	
160.0000	.9171	
162.5000	.9245	
165.0000	.9315	
167.5000	.9379	
170.0000	.9434	
172.5000	.9479	
175.0000	.9512	
177.5000	.9533	
180.0000	.9540	
.9254	-.0625	.0911
1.0000	-.0675	.0985
.0908	.1687	.0373

APPENDIX B

The program described in this appendix was also used in the analysis of the angular correlation data. The method is due to White (12).

This program uses the data at the three points, 90^{o}, 135^{o} and 180^{o}, to solve the system of three equations

$$W(\theta_i) = C_0 + C_2P_2 (\cos \theta_i) + C_4P_4 (\cos \theta_i) \; ; \; i = 1, 2, 3.$$

This gives the three coefficients C_0, C_2, and C_4 directly. The statistical errors in these coefficients are also calculated.

The number of coincidence counts, with background subtracted, is entered as input data for the program. This data is entered in Format F5.4.

Consider the sample output given on the page following the program. The first line gives the input data as in the previous program. The data is not normalized as in the previous program. The coefficients C_0, C_2, and C_4 are typed out, followed by their normalized values. The statistical errors in these coefficients are then given. As in the previous program, the coefficients C_0, C_2, and C_4 are used to compute the best fit curve. The angles and the corresponding values of $W(\theta)$ are typed out for the angular range, 90^{o} to 180^{o} at 5^{o} intervals.

```
*FANDK1604
ZZFORX51
      K=0
      D=176.
   10 READ 1,A
      READ 1,B
      READ 1,C
    1 FORMAT (F5.4)
      PUNCH 2,A,B,C
    2 FORMAT (3F12.4)
      AA=(.009524)*((42.*A)+(56.*B)+(7.*C))
      AB = (.009524)*((-90.*A)+(40.*B)+(50.*C))
      AC = (.009524)*((48.*A)-(96.*B)+(48.*C))
      PUNCH 2,AA,AB,AC
      A2=AB/AA
      A4=AC/AA
      CALL PLOT (1,90.,180.,4.5,2.5,.5,1.5,10.,.1)
      A = A+D
      B=B+D
      C=C+D
      A2N1=A*(90.+(42.*A2))*(90.+(42.*A2))
      A2N2=B*(40.-(56.*A2))*(40.-(56.*A2))
      A2N3=C*(50.-(7.*A2))*(50.-(7.*A2))
      A2NS=SQRTF(A2N1+A2N2+A2N3)
      A2E=(1./(105.*AA))*A2NS
      A4N1=A*(48.-(42.*A4))*(48.-(42.*A4))
      A4N2=B*(96.+(56.*A4))*(96.+(56.*A4))
      A4N3=C*(48.-(7.*A4))*(48.-(7.*A4))
      A4NS=SQRTF(A4N1+A4N2+A4N3)
      A4E=(1./(105.*AA))*A4NS
      PUNCH 3,A2,A4
    3 FORMAT (2F10.4)
      PUNCH 3,A2E,A4E
      AT=1.-(1./2.)*A2+(3./8.)*A4
      BU=(3./2.)*(A2-((5./2.)*(A4)))
      CV=(35./8.)*A4
      PUNCH 2,AT,BU,CV
      BB=85.
   11 BB=BB+5.
      BBR = BB*6.2832/360.
      BBRC = COSF(BBR)
      BBRD = BBRC*BBRC
      AYC = AT+(BU*BBRD)+(CV*BBRD*BBRD)
      PUNCH  8,BB,AYC
    8 FORMAT(2F10.4)
      CALL PLOT (9,BB,AYC)
      IF (BB-180.) 11,13,13
   13 CONTINUE
      CALL PLOT(7)
      K=K+1
      GO TO (10,10,10,15,10,10,10,12,14),K
   15 D=30.
      GO TO 10
   12 D = 45.
      GO TO 10
   14 CALL EXIT
      END
1
```

```
  785.0000     748.0000     706.0000
  760.0152     -51.7153      -2.2857
  -.0680     -.0030
   .0387      .0410
    1.0328       -.0907       -.0131
 90.0000     1.0328
 95.0000     1.0322
100.0000     1.0301
105.0000     1.0267
110.0000     1.0220
115.0000     1.0162
120.0000     1.0093
125.0000     1.0016
130.0000      .9931
135.0000      .9842
140.0000      .9750
145.0000      .9660
150.0000      .9574
155.0000      .9494
160.0000      .9424
165.0000      .9367
170.0000      .9324
175.0000      .9298
180.0000      .9289
```

REFERENCES

1. Hamilton, D.R., Phys. Rev. 58, 122, (1940)

2. Siegbahn, K., "Alpha, Beta, and Gamma Ray Spectroscopy", Volume 2, (North Holland Publishing Company), (1965)

3. Biedenharn, L. C., and Rose, M. E., Rev. of Mod. Phys. 25, 729, (1953)

4. Ferentz, H., and Rosensweig, N., Argonne National Laboratory Report 5324 (1954) and published in "Alpha, Beta, and Gamma Ray Spectroscopy", edited by K. Siegbahn (North Holland Publishing Company)

5. Rose, M. E., Biedenharn, L. C., and Arfken, G. B., Phys. Rev. 88, 5, (1952)

6. Alburger, D. E., and Sunyar, A. W., Phys. Rev. 99, 695, (1955)

7. Rose, M. E., Internal Conversion Coefficients (1958) (North Holland Publishing Company)

8. Kurey, T. J., and Roy, R. R., Nuclear Phys. 44, 670, (1963)

9. Kelly, W. H., and Horen, D. J., Nuclear Phys. 47, 454, (1963)

10. Cork, J. M., Leblanc, J. M., Nester, W. H., and Brice, M. K., Phys. Rev. 91, 76, (1953)

11. Brundrit, D. R., and Sen, S. K., Nuclear Phys. 68, 287, (1965)

12. White, D. H., Nuclear Inst. and Methods, 21, 209, (1963)

13. Yates, M. J. L., "Alpha, Beta, and Gamma Ray Spectroscopy" (1965) edited by K. Siegbahn (North Holland Publishing Company)